Struct Chem (2016) 27:1041–1047
DOI 10.1007/s11224-015-0703-8

ORIGINAL RESEARCH

Density functional theory study of the regio- and stereoselectivity of 1,3-dipolar cycloaddition reactions between 2-ethylthio-4-phenyl-1-azetin and some substituted nitrile oxides

Amir Khojastehnezhad[1] · Hossein Eshghi[1] · Farid Moeinpour[2] · Mehdi Bakavoli[1] · Mohammad Izadyar[1] · Javad Tajabadi[1]

Received: 9 October 2015 / Accepted: 11 November 2015 / Published online: 24 November 2015

Abstract The mechanism (regio- and stereoselectivity) of 1,3-dipolar cycloaddition (1,3-DC) of 2-ethylthio-4-phenyl-1-azetin **1** with benzonitrile oxide **2a**, 2-aminobenzonitrile oxide **2b** and 2-azidobenzonitrile oxide **2c** has been investigated by density functional theory-based reactivity indices and activation energy calculations at B3LYP/6-31G(d,p) level of theory in the gas and solvent phase. Thermodynamic and kinetic parameters of the possible *ortho*/*meta* regioisomeric and *endo*/*exo* stereoisomeric pathways have been determined. In order to rationalize complete *endo* selective fashion provided by these 1,3-DC cycloadditions, a natural steric analysis between NLMOs i,j for **TS1ox** and **TS1on** and also a second-order interaction energy, E^2, analysis between the donor–acceptor orbitals in these TSs were carried out. In all cases, the *ortho* pathways are more favorable compared to the *meta* alternatives and it is found that the *endo* pathway is preferred. Our results show that these cycloadditions follow an asynchronous one-step mechanism with a nonpolar character. Theoretical data are in good agreement with the experimental results.

Keywords Regioselectivity · Stereoselectivity · 1,3-Dipolar cycloaddition · 2-ethylthio-4-phenyl-1-azetin · DFT reactivity indices

Introduction

The cycloaddition reactions play a fundamental role in organic synthesis and mechanistic studies [1]. The 1,3-DC reaction, which is the joining of a 1,3-dipole with a dipolarophile, is an efficient way for the synthesis of five-membered heterocyclic structures [2–4]. In particular, the nitrile oxides are the important dipoles which react with double carbon–nitrogen bonds and afforded the 1,2,4-oxadiazole [5, 6]. These aromatic rings have various biological and medical applications [7, 8] and have been introduced into drug discovery programs for several different purposes. In some cases, they have been used as potent EthR inhibitors that boost ethionamide activity in the treatment of multi-drug-resistant tuberculosis [9]. In other cases, oxadiazoles have been displayed to act as a flat, aromatic linker to put substituents in the suitable position [10] and also regulating molecular properties by positioning them in the periphery of the molecule [11]. They have also been used as replacements for carbonyl including compounds like esters, amides, carbamates and hydroxamic esters [12, 13].

The 1,3-DC reactions have customarily been studied by the frontier molecular orbital (FMO) theory and transition state theory (TST). Although TST remains the most greatly used and the most rigorous approach for the investigation of the mechanism of these reactions, the transition state locating is not always more comfortable. Furthermore, transition state calculations often require a lot of time when big substituents are existent in reactive systems. The reactivity indexes, as described by the density functional

Electronic supplementary material The online version of this article (doi:10.1007/s11224-015-0703-8) contains supplementary material, which is available to authorized users.

✉ Hossein Eshghi
heshghi@um.ac.ir

✉ Farid Moeinpour
f.moeinpour@gmail.com; fmoeinpour52@iauba.ac.ir

[1] Department of Chemistry, Faculty of Sciences, Ferdowsi University of Mashhad, Mashhad, Iran

[2] Department of Chemistry, Faculty of Sciences, Bandar Abbas Branch, Islamic Azad University, Bandar Abbas 7915893144, Iran

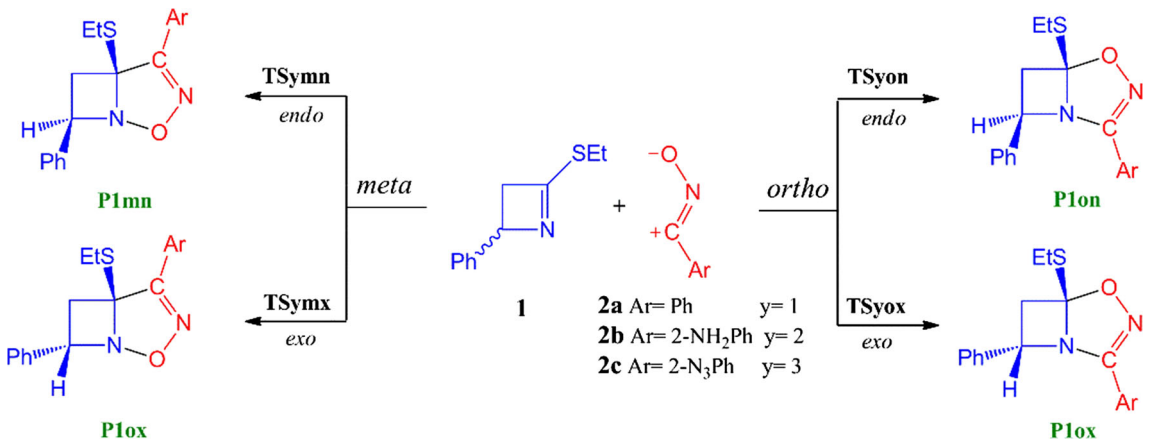

Scheme 1 Regio- and stereoisomeric pathways for the investigated 1,3-dipolar cycloadditions

theory (DFT) [14], such as Fukui indices, local softnesses and local electrophilicity, have been used to rationalize the reactivity and regiochemistry of cycloaddition reactions [15–17]. For instance, several treatments of 1,3-DC reactions of nitrile oxide with various dipolarophiles can be found in the literature [18–20]. In continuation of our previous works on the theoretical investigation of 1,3-DC reactions [21–28], we present the results of an extended investigation on the reactivity, regio- and stereoselectivity of 1,3-DC reaction between 2-ethylthio-4-phenyl-1-azetin **1** with benzonitrile oxide **2a**, 2-aminobenzonitrile oxide **2b** and 2-azidobenzonitrile oxide **2c** based on activation energy calculations and DFT-based reactivity indices. Experimentally, it has been found that the cycloaddition reactions of **1** with **2a**, **2b** and **2c** give only (5R,7R)-5-(ethylthio)-2-aryl-7-phenyl-4-oxa-1,3 diazabicyclo[3.2.0]hept-2-ene **P1on** as shown in Scheme 1. These results showed that the *ortho* and *endo* pathways are dominant [29].

Computational methods

All calculations were done with GAUSSIAN03 program package [30]. Geometric optimization of the reactants was done by DFT methods at the B3LYP/6-31G (d,p) level of theory [31]. The transition states (TSs) for the 1,3-DC reactions have been localized at the B3LYP/6-31G(d,p) level of theory. Frequency calculations described the stationary points to confirm that the TSs had one and only one imaginary frequency. The intrinsic reaction coordinates (IRC) [32] calculation was done in forward and backward path to determine that each saddle point joints to the two related minima by the second-order González–Schlegel integration method [33, 34]. Solvent effects were considered at the B3LYP/6-31G (d,p) level of theory by geometry optimization of the gas-phase structures using a self-consistent reaction field (SCRF) [35] on the basis of the polarizable continuum model (PCM) of Tomasi's group [36]. Because the studied cycloaddition reactions were carried out in diethyl ether, we selected its dielectric constant at 298.0 K, $\varepsilon = 4.3$. The electronic chemical potential μ was assessed in terms of the one electron energy of the HOMO and LUMO, using Eq. (1) [37]:

$$\mu = (\varepsilon_H + \varepsilon_L)/2 \quad (1)$$

The global electrophilicity ω for dipoles and dipolarophile was determined using Eq. (2) [38]:

$$\omega = \mu^2/2(\varepsilon_L - \varepsilon_H) \quad (2)$$

The global nucleophilicity index N [39], based on the HOMO energies obtained within the Kohn–Sham scheme [40], is defined as $N = \varepsilon_{HOMO}$ (Nu) $- \varepsilon_{HOMO}$ (TCE) in which (Nu) denotes nucleophile. This relative nucleophilicity index refers to tetracyanoethylene (TCE).

Results and discussion

Theoretical studies of the regio- and stereochemistry of these 1,3-DC reactions will be based on two sections. Firstly, we focus our attention on the energetic aspects of the 1,3-DC reactions. In the second section, we investigate the bond lengths, bond orders, steric analysis and charge transfers in the TS structures.

Activation energy calculations

In this present study, the transition states are located through vibrational frequency analysis. Each such transition state is distinguished by a single imaginary frequency. There are two regioisomeric pathways—*ortho* and *meta*—and two stereoisomeric pathways—*endo* and *exo*—as shown in Scheme 1. For the different structures of the nearing reactants, transition states and the products, a useful naming

system has been utilized according to our previous theoretical investigations [21, 22, 26, 27]. Abbreviated structural symbols for the products (**Pyon**, **Pyox**, **Pymn**, **Pymx**), the transition states (**TSyon**, **TSyox**, **TSymn**, **TSymx**) and the oriented reactants (**1**, **2a**, **2b**, **2c**) have been followed throughout this discussion. In these reactions, cycloadditions of dipolarophile **1** with nitrile oxides (**2a**, **2b**, **2c**) in *ortho* channel and *endo/exo* stereoselectivity approach lead to products **Pyon** and **Pyox**. Similarly, cycloaddition reactions of dipolarophile **1** with nitrile oxides (**2a**, **2b**, **2c**) with *meta* channel and *endo/exo* stereoselectivity approach lead to products **Pymn** and **Pymx**. The transition states **TSyon**, **TSyox**, **TSymn** and **TSymx** are related to products **Pyon**, **Pyox**, **Pymn** and **Pymx,** respectively, and also, $y = 1, 2$ and 3 are used for (**2a**, **2b** and **2c**) nitrile oxide derivatives, respectively (Scheme 1).

The corresponding activation barriers, structures and energy profile are given in Table 1, Figs. 1 and 2, respectively. All the reactions progressed exothermically with large ΔH values (Table 1). In accord with Hammond's postulate, the TSs should then be more adjacent to the reactants. As shown in Table 1, for the all these reactions, the *ortho* cyclization modes are more favorable than the *meta* ones by about 17 kcal mol^{-1}, leading to the formation of the *ortho* cycloadducts **Pyon** and **Pyox**, while the *endo* approach modes giving **P1on**, **P2on** and **P3on** are more favorable, by ca. 2 kcal mol^{-1}, than the *exo* ones. Moreover, in order to confirm our calculations, we calculated above activation energies for reaction between **1** and **2a** with larger basis set (6 − 311 + G(2d,p)), we obtained same results. Therefore, 1,3-DC reactions show complete *ortho* regioselectivity and high *endo* stereoselectivity. These results are in agreement with the experimental data [29].

In order to rationalize complete *endo* selectivity along *ortho* regioisomeric pathway, a natural steric analysis was carried out on the B3LYP/6-31G (d,p)-generated wave function of both optimized **TS1on** and **TS1ox** (as a model) using Gen NBO5.0 W software [41]. Important pairwise steric exchange energies, $\Delta E_{i,j}$, between NLMOs i,j for **TS1on** and **TS1ox** in 1,3-DC reaction of **1** toward **2a** including optimized structures of **TS1on** and **TS1ox** together with corresponding atoms numbering are given in Table S1 from supplementary information. As shown, the sum of important pairwise steric exchange energies is 288.99 and 299.11 kcal mol^{-1} for **TS1on** and **TS1ox**, respectively, indicating that **TS1ox** suffers from a larger destabilizing steric interaction than **TS1on** about 10.12 kcal mol^{-1}. The greatest value of pairwise steric exchange energy in both **TS1ox** and **TS1on** is associated with the interaction between σ C1–C5/σ C8-N14 and σ C1–C5/σ C8-N13, respectively (see Table S1 from supplementary information). In order to complete the study of *endo* selectivity provided by the 1,3-DC reaction of **1** toward **2a**, stabilizing electron density delocalization effects were also examined.

Table 1 Relative Gibbs free energies (ΔG, in kcal mol^{-1}) and enthalpies (ΔH, in kcal mol^{-1}) computed at 298.15 K and 1 atm in the gas phase and diethyl ether for the transition states (TSs) and cycloadducts (CAs) involved in the 1,3-DC reactions of **1** with **2a**, **2b** and **2c**

	Gas phase		Solvent			Gas phase		Solvent	
	ΔH	ΔG	ΔH	ΔG		ΔH	ΔG	ΔH	ΔG
TS1on[a]	12.51	26.21	13.63	27.16	**CA1on**[a]	−43.79	−41.88	−43.35	−41.52
TS1ox[a]	13.57	27.87	14.16	28.40	**CA1ox**[a]	−42.72	−40.68	−42.10	−40.21
TS1mn[a]	29.87	43.32	30.85	44.16	**CA1mn**[a]	−33.32	−31.28	−32.75	−30.52
TS1mx[a]	32.03	46.51	33.20	47.21	**CA1mx**[a]	−30.70	−29.14	−30.69	−28.81
TS1on[b]	16.53	29.88	17.65	30.81	**CA1on**[b]	−40.39	−38.37	−39.97	−38.02
TS1ox[b]	17.74	31.45	18.36	32.03	**CA1ox**[b]	−39.36	−36.95	−38.72	−36.46
TS1mn[b]	35.52	49.28	36.57	50.15	**CA1mn**[b]	−31.44	−29.87	−30.87	−29.11
TS1mx[b]	38.17	52.34	39.32	53.05	**CA1mx**[b]	−29.37	−27.64	−29.11	−27.29
TS2on[c]	12.19	26.03	13.77	27.11	**CA2on**[c]	−45.60	−43.35	−44.63	−42.02
TS2ox[c]	13.29	27.89	14.43	28.40	**CA2ox**[c]	−44.36	−42.30	−43.41	−41.25
TS2mn[c]	30.15	43.66	31.15	44.87	**CA2mn**[c]	−35.370	−32.97	−33.97	−31.82
TS2mx[c]	31.53	46.75	33.12	49.00	**CA2mx**[c]	−30.96	−30.82	−31.48	−30.99
TS3on[d]	13.47	27.10	14.54	27.67	**CA3on**[d]	−41.68	−39.44	−41.60	−39.09
TS3ox[d]	14.84	29.07	15.33	29.77	**CA3ox**[d]	−41.17	−39.05	−40.71	−38.84
TS3mn[d]	30.14	43.41	31.67	45.60	**CA3mn**[d]	−29.85	−27.53	−30.27	−28.70
TS3mx[d]	32.77	47.34	33.94	48.39	**CA3mx**[d]	−27.73	−26.31	−28.23	−26.68

[a] Relative to **1** + **2a** at 6-31G (d,p)

[b] Relative to **1** + **2a** at 6-311G+ (2d,p)

[c] Relative to **1** + **2b**

[d] Relative to **1** + **2c**

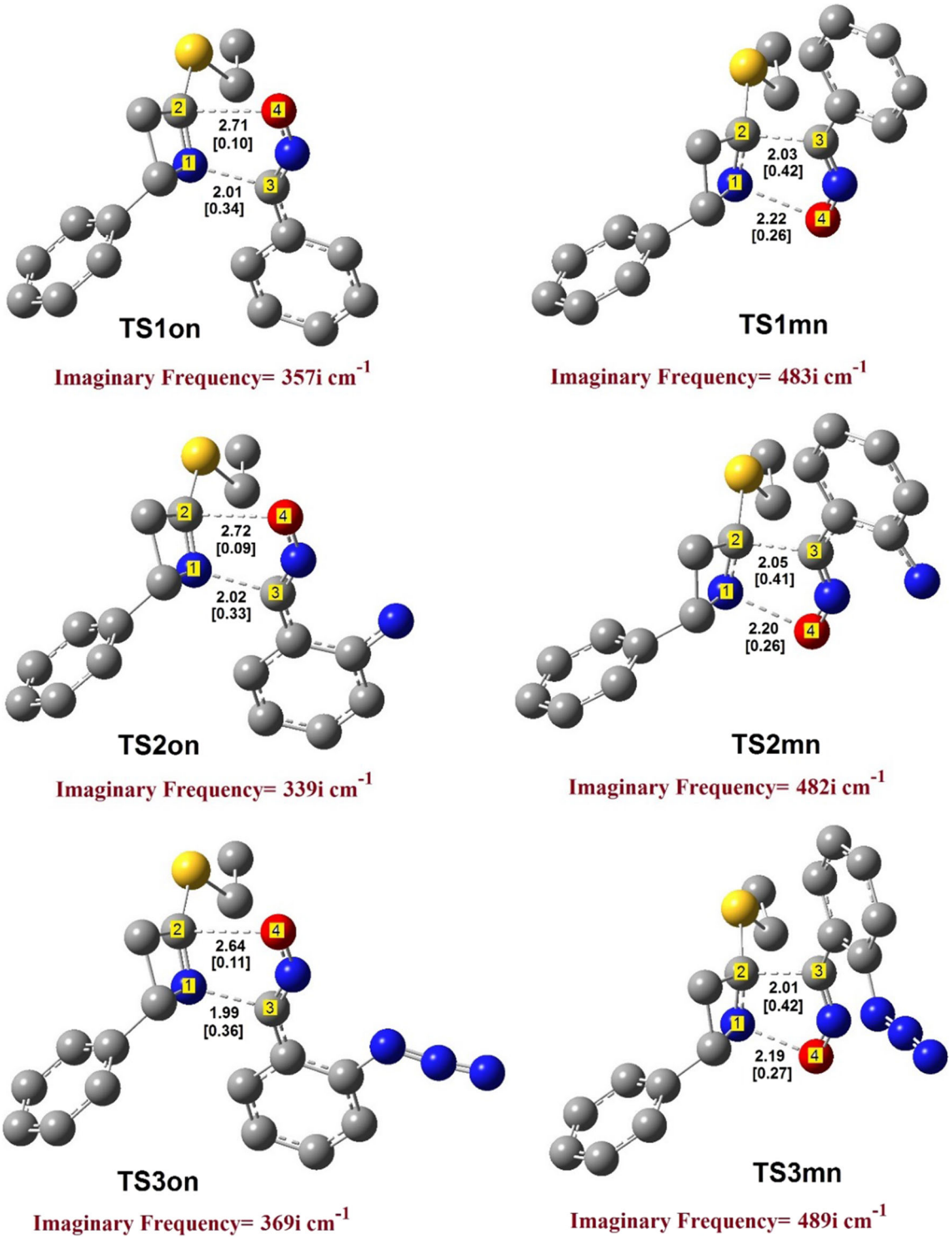

Fig. 1 Optimized geometries for the transition state structures at the B3LYP/6-31G (d,p) level of theory. Hydrogen atoms have been omitted for clarity. Distances of forming bonds are given in angstroms. The bond orders are given in *brackets*

Delocalization of electron density between occupied Lewis-type (bond or lone pair) NBO orbitals and formally unoccupied (anti-bond or Rydberg) non-Lewis NBO orbitals corresponds to a stabilizing donor–acceptor interaction. The energy of this interaction can be estimated by the second-order perturbation theory [42]. The calculated important second-order interaction energies (E^2) between the donor–acceptor orbitals in **TS1ox** and **TS1on** as well as

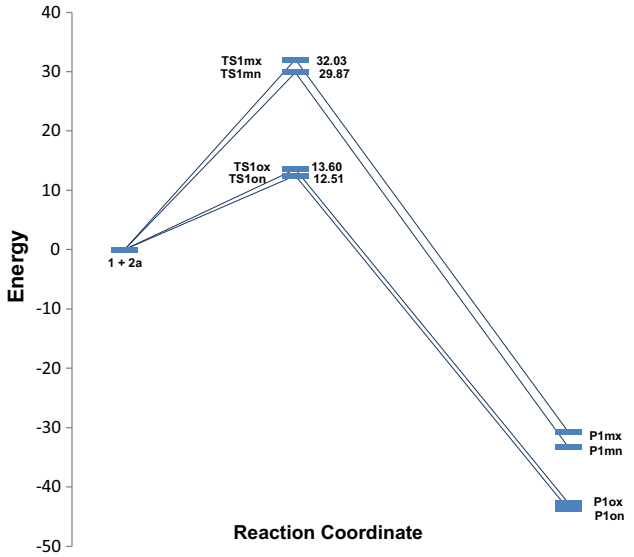

Fig. 2 Energy profile in kcal mole^{-1} for the 1,3-DC reaction between dipolarophile **1** and dipole **2a**

optimized structures of these TSs together with corresponding atoms numbering are listed in Table S2 from supplementary information. As presented in this table, the sum of important second-order interaction energies is 485.02 and 477.74 kcal mol^{-1} for **TS1on** and **TS1ox**, respectively. These values obviously show that **TS1on** is stabilized than **TS1ox** by 7.28 kcal mol^{-1} explaining the preferable *endo* selectivity displayed by the studied 1,3-DC reaction. It is interesting to note that the greatest value of the second-order interaction energy in **TS1ox** and **TS1on** is related to the delocalization of donor LP (3) O4 to the acceptor π* C2–N3 and donor LP (2) S9 to the acceptor π* C1–N13, respectively.

As the 1,3-DC reactions between dipolarophile **1** and dipoles **2a**, **2b** and **2c** were carried out in diethyl ether, which can have some prevalence on the energies and geometries, solvent effects in these 1,3-DC reactions were evaluated by full optimization of the solvent phase geometries by utilizing the PCM model of Tomasi's group [36]. The relative energies are summarized in Table 1. With the incorporation of solvent effects, reactants are more stabilized than TSs and Ps [43]. As a result, in diethyl ether, the relative Gibbs free energies associated with *ortho* and *meta* TSs are moderately increased between 0.5–1.1 and 0.7–2.2 kcal mol^{-1}, respectively (Table 1).

The geometries of the TSs, the lengths of the C–O, C–N, C–C and N–O forming bonds and their Wiberg bond order values involved in these 1,3-DC reactions are shown in Fig. 1. Analysis of the lengths of the two forming bonds in the TSs shows that they are not formed to the same extent. It is of note that the C–N bond length is shorter than the C–O bond length (in **TS1on**, **TS2on** and **TS3on**) and C–C bond is shorter than N–O bond (in **TS1mn**, **TS2mn** and **TS3mn**). The degree of bond formation on a reaction path is given by the bond order conception [44]. The bond order (Wiberg indices) values of the C–O, C–N, C–C and N–O forming bonds at TSs are shown in square brackets in Fig. 1. These values are within the range of 0.09–0.36 for favorable pathway (**TS1on**, **TS2on** and **TS3on**) and 0.26–0.42 for unfavorable pathway (**TS1mn**, **TS2mn** and **TS3mn**). The differences of bond order for forming bonds at the TSs indicate asynchronous one-step mechanism processes. These results also show that the most favorable TSs (**TS1on**, **TS2on** and **TS3on**) are consistently more asynchronous than the unfavorable ones (**TS1mn**, **TS2mn** and **TS3mn**).

Recently, an interesting and helpful classification for Diels–Alder (DA) reactions based on the polar character, global electron density transfer (GEDT) computed at the TS, of DA reaction between cyclopentadiene and twelve substituted ethylenes has been provided by Domingo et al. [45]. According to this classification, there are three different types of DA reactions: (a) nonpolar DA (*N*-DA) reactions for which GEDT and activation energy are less than 0.15e and higher than 18 kcal mol^{-1}, respectively; (b) polar DA (*P*-DA) reactions which are characterized by 0.15e < GEDT < 0.40e and an activation energy ranging from 17 to 5 kcal mol^{-1}; (c) and finally, ionic DA (*I*-DA) reactions show a GEDT higher than 0.40e and negative activation energy. Therefore, the electronic nature of these 1,3-DC reactions is evaluated by analyzing the global electron density transfer at the TSs along the cycloaddition process. In the gas phase, the GEDTs at the TSs, which passes from the dipolarophile to the dipole moiety, are 0.123 e, 0.130 e and 0.122 e for the favorable TSs **TS1on**, **TS2on** and **TS3on,** respectively, indicating nonpolar character for these 1,3-DC reactions. This low electron density transfer can be related to the electron-rich character of the dipolarophile **1**.

IRC calculations were carried out for all studied reactions and presented only for the reaction pathway leading to **P1on** (Figure S1 from supplementary information). This figure shows saddle point clearly and illustrates that the TSs connect to the associated minima of the concerted mechanism.

DFT-based reactivity indices

HOMO and LUMO energies, electronic chemical potential μ, chemical hardness η, global electrophilicity ω and global nucleophilicity N of the dipolarophile **1** and nitrile oxides **2a**, **2b** and **2c** are given in Table 2.

As it can be seen in Table 2, the electronic chemical potential (μ) of dipolarophile **1** (−0.1165) is greater than those of dipoles **2a** (−0.1409), **2b** (−0.1248) and **2c**

Table 2 HOMO and LUMO energies in a.u., electronic chemical potential (μ in a.u.), chemical hardness (η in a.u.), global electrophilicity (ω, in eV) and global nucleophilicity (N, in eV) for reactants **1**, **2a**, **2b** and **2c**

Reactants	ε_{HOMO}	ε_{LUMO}	μ	η	ω	N[a]
1	−0.2308	−0.0023	−0.1165	0.2285	0.8088	2.8409
2a	−0.2331	−0.0487	−0.1409	0.1844	1.4648	2.7783
2b	−0.2107	−0.039	−0.1248	0.1717	1.2352	3.3878
2c	−0.2307	−0.0599	−0.1453	0.1708	1.6818	2.8436

[a] HOMO energy of tetracyanoethylene is −0.3351 a.u. at the same level of theory

(−0.1453), which shows that the charge transfer takes place from dipolarophile **1** to dipoles **2a**, **2b** and **2c**. Consequently, the dipoles **2a**, **2b** and **2c** can act as electrophile in these 1,3-DC reactions. These results are in agreement with GEDT calculations at the TSs. The electrophilicity difference for the dipole/dipolarophile pair, $\Delta\omega$, is a useful criterion to describe the high- or low-polar nature of the cycloaddition [46]. The small $\Delta\omega$ between **1** and **2a**, **2b** and **2c** is 0.66, 0.42 and 0.87 eV, respectively, which shows a nonpolar character for these 1,3-DC reactions.

A useful classification of 1,3-DC reactions into *pseudodiradical-type* (*pr-type*) and *zwitterionic-type* (*zw-type*) reactions has been proposed [47]. *Pr-type* reactions occur easily via an earlier TS with nonpolar nature, and *zw-type* reactions occur via polar TSs. It can be concluded that our investigated reactions participate in *pr-type* reactions. Recently, Domingo proposed the new local reactivity, Parr functions, in polar organic reactions [48]. In the present study, dipolarophile **1** is not electrophilically motivated; consequently, these 1,3-DC reactions are nonpolar. Therefore, Parr functions cannot give correct information about the regioselectivity in these nonpolar 1,3-DC reactions. He declared that due to the electrophilic/nucleophilic manner of these reactions, the Fukui functions on the basis of finite charge differentiations cause some serious errors and are not match to exchange in charge distribution, as suggested by these Fukui functions. Therefore, the Fukui functions also could not be used.

Conclusion

The 1,3-DC reaction of 2-ethylthio-4-phenyl-1-azetin and nitrile oxide derivatives has been investigated at DFT/B3LYP/6-31G(d,p) level of the theory in the gas and diethyl ether phases. The computed energies, enthalpies and free energies of activation of the transition states indicated experimentally formed products from *ortho* regioisomeric channels and *endo* stereoisomeric approaches along the *ortho* pathways are more favorable cycloadducts. Wiberg bond index and GEDT indicated an asynchronous one-step mechanism over the regioisomeric reaction channels. In order to rationalize complete *endo* selective fashion provided by these 1,3-DC cycloadditions, a natural steric analysis between NLMOs i,j for **TS1ox** and **TS1on** and also a second-order interaction energy, E^2, analysis between the donor–acceptor orbitals in these TSs were carried out. The results evidently showed that the complete *endo* selectivity explained **TS1on** leads the *endo* stereoisomeric approach preferred over the *exo* one.

Acknowledgments The financial support for this work was provided by Research Council of Ferdowsi University of Mashhad (Grant No. 3/29765) and Islamic Azad University, Bandar Abbas Branch.

References

1. Padwa A, Pearson WH (2003) Synthetic applications of 1, 3-dipolar cycloaddition chemistry toward heterocycles and natural products, vol 59. Wiley, New York
2. Huisgen R (1963) Angew Chem Int Ed Eng 2:565
3. Padwa A (2002) 1, 3-Dipolar cycloaddition chemistry, vol 1. Wiley, New York
4. Gothelf KV, Jørgensen KA (1998) Chem Rev 98:863
5. Nishiwaki N, Kobiro K, Hirao S, Sawayama J, Saigo K, Ise Y, Okajima Y, Ariga M (2011) Org Biomol Chem 9:6750
6. Kumar RS, Ramar A, Perumal S, Almansour AI, Arumugam N, Ali MA (2013) Synth Commun 43:2763
7. Boström J, Hogner A, Llinàs A, Wellner E, Plowright AT (2012) J Med Chem 55:1817
8. Scott JS, Birch AM, Brocklehurst KJ, Broo A, Brown HS, Butlin RJ, Clarke DS, Davidsson Ö, Ertan A, Goldberg K, Groombridge SD, Hudson JA, Laber D, Leach AG, MacFaul PA, McKerrecher D, Pickup A, Schofield P, Svensson PH, Sörme P, Teague J (2012) J Med Chem 55:5361
9. Villemagne B, Crauste C, Flipo M, Baulard AR, Déprez B, Willand N (2012) Eur J Med Chem 51:1
10. Ono M, Haratake M, Saji H, Nakayama M (2008) Bio Med Chem 16:6867
11. Orlek BS, Blaney FE, Brown F, Clark MSG, Hadley MS, Hatcher J, Riley GJ, Rosenberg HE, Wadsworth HJ, Wyman P (1991) J Med Chem 34:2726
12. Warmus JS, Flamme C, Zhang LY, Barrett S, Bridges A, Chen H, Gowan R, Kaufman M, Sebolt-Leopold J, Leopold W, Merriman R, Ohren J, Pavlovsky A, Przybranowski S, Tecle H, Valik H, Whitehead C, Zhang E (2008) Bioorg Med Chem Lett 18:6171
13. McBriar MD, Clader JW, Chu I, Del Vecchio RA, Favreau L, Greenlee WJ, Hyde LA, Nomeir AA, Parker EM, Pissarnitski DA, Song L, Zhang L, Zhao Z (2008) Bioorg Med Chem Lett 18:215

14. Ess DH, Jones GO, Houk K (2006) Adv Synth Catal 348:2337
15. Le TN, De Proft F, Chandra AK, Langenaeker W, Nguyen MT, Geerlings P (1999) J Am Chem Soc 121:5992
16. Nguyen LT, Proft FD, Chandra AK, Uchimaru T, Nguyen MT, Geerlings P (2001) J Org Chem 66:6096
17. Chandra AK, Nguyen MT (1998) J Phys Chem A 102:6181
18. Shang YJ, Wang YG (2002) Synthesis 1663
19. Shankar BB, Yang DY, Girton S, Ganguly AK (1998) Tetrahedron Lett 39:2447
20. Kang KH, Pae AN, Choi KL, Cho YS, Chung BY, Lee JE, Jung SH, Koh HY, Lee HY (2001) Tetrahedron Lett 42:1057
21. Moeinpour F, Khojastehnezhad A (2014) J Iran Chem Soc 11:1459
22. Rahimizadeh M, Eshghi H, Khojastehnezhad A, Moeinpour F, Bakavoli M, Tajabadi J (2014) J Fluor Chem 162:60
23. Moeinpour F, Bakavoli M, Davoodnia A, Morsali A (2012) J Theo Comput Chem 11:99
24. Bakavoli M, Moeinpour F, Davoodnia A, Morsali A (2010) J Mol Struct 969:139
25. Moeinpour F (2010) Chin J Chem Phys 23:165
26. Eshghi H, Khojastehnezhad A, Moeinpour F, Bakavoli M (2015) Can J Chem 93:749
27. Moeinpour F, Khojastehnezhad A (2015) Acta Chim Slov 62:403
28. Emamian S, Lu T, Moeinpour F (2015) RSC Adv 5:62248
29. Hemming K, Khan MN, O'Gorman PA, Pitard A (2013) Tetrahedron 69:1279
30. Cheeseman JR, Montgomery JA, Vreven T, Kudin KN, Burant JC, Millam JM, Iyengar SS, Tomasi J, Barone V, Mennucci B, Cossi M, Scalmani G, Rega N, Petersson GA, Nakatsuji H, Hada M, Ehara M, Toyota K, Fukuda R, Hasegawa J, Ishida M, Nakajima T, Honda Y, Kitao O, Nakai H, Klene M, Li X, Knox JE, Hratchian HP, Cross JB, Bakken V, Adamo C, Jaramillo J, Gomperts R, Stratmann RE, Yazyev O, Austin AJ, Cammi R, Pomelli C, Ochterski JW, Ayala PY, Morokuma K, Voth GA, Salvador P, Dannenberg JJ, Zakrzewski VG, Dapprich S, Daniels AD, Strain MC, Farkas O, Malick DK, Rabuck AD, Raghavachari K, Foresman JB, Ortiz JV, Cui Q, Baboul AG, Clifford S, Cioslowski J, Stefanov BB, Liu G, Liashenko A, Piskorz P, Komaromi I, Martin RL, Fox DJ, Keith T, Al-Laham MA, Peng CY, Nanayakkara A, Challacombe M, Gill PMW, Johnson B, Chen W, Wong MW, Gonzalez C, Pople JA (2003) Gaussian 03, revision B. 03. Gaussian Inc., Pittsburgh
31. Schlegel HB (1982) J Comput Chem 3:214
32. Head-Gordon M, Pople JA (1988) J Chem Phys 89:5777
33. Gonzalez C, Schlegel HB (1990) J Phys Chem 94:5523
34. Gonzalez C, Schlegel HB (1991) J Chem Phys 95:5853
35. Tomasi J, Persico M (1994) Chem Rev 94:2027
36. Cances E, Mennucci B, Tomasi J (1997) J Chem Phys 107:3032
37. Parr RG, Pearson RG (1983) J Am Chem Soc 105:7512
38. Parr RG, Szentpaly LV, Liu S (1999) J Am Chem Soc 121:1922
39. Domingo LR, Chamorro E, Pérez P (2008) J Org Chem 73:4615
40. Galli G (1996) Curr Opin Solid State Mater Sci 1:864
41. Glendening ED, Badenhoop JK, Reed AE, Carpenter JE, Bohmann JA, Morales CM, Weinhold F (2001) NBO 5.0. Theoretical Chemistry Institute, University of Wisconsin, Madison
42. Reed AE, Curtiss LA, Weinhold F (1988) Chem Rev 88:899
43. Benchouk W, Mekelleche SM, Silvi B, Aurell MJ, Domingo LR (2011) J Phys Org Chem 24:611
44. Wiberg KB (1968) Tetrahedron 24:1083
45. Domingo LR, Sáez JA (2009) Org Biomol Chem 7:3576
46. Chemouri H, Mekelleche SM (2012) Int J Quantum Chem 112:2294
47. Domingo LR, Emamian SR (2014) Tetrahedron 70:1267
48. Domingo LR, Pérez P, Sáez JA (2013) RSC Adv 3:1486